ELSEVIER

Surface Science 443 (1999) 105–115

surface science

www.elsevier.nl/locate/susc

Atom and cluster diffusion on Re(0001)

J.T. Goldstein *, G. Ehrlich

Materials Research Laboratory and Department of Physics, University of Illinois at Urbana-Champaign, Urbana, IL 61801, USA

Received 21 June 1999; accepted for publication 26 August 1999

Abstract

Diffusion of Re and W adatoms and Re clusters has been surveyed on the close-packed (0001) surface of rhenium, the first study of atom motion on an hcp metal. From the temperature dependence of the diffusivity, the activation energies to diffusion are found to be 11.11 ± 0.43 and 11.04 ± 0.34 kcal mol^{-1} for Re and W adatoms. The respective prefactors amount to $6.13(\times 2.6^{\pm 1}) \times 10^{-6}$ and $2.17(\times 2.7^{\pm 1}) \times 10^{-3}$ cm^2 s^{-1}. The energy barrier for single adatom motion over the step edge is estimated to be 15.7 ± 0.4 and 19.3 ± 0.4 kcal mol^{-1} for Re and W. Before descending the step edge, the adatoms become trapped at the edge, and have to overcome a barrier of ~ 13 kcal mol^{-1} to return to the plane's center. The behavior of clusters containing from two to eight Re atoms has also been examined. Rotational Brownian motion is observed for Re_4 under the influence of a strong imaging field. The activation energies for diffusion of Re clusters on Re(0001) are found to bear a striking resemblance to those of Ir clusters on the Ir(111) surface. Comparison of single atom diffusion on Re(0001) with that on other densely packed surfaces reveals that the diffusion barriers do not scale quantitatively with the cohesive energy.

Keywords: Adatoms; Clusters; Rhenium; Single crystal surfaces; Surface diffusion

1. Introduction

Since the diffusion of individual metal adatoms first became amenable to detailed study through the use of the field ion microscope, quite a number of surfaces on bcc as well as fcc crystals have been successfully examined [1]. Recently, because of growing interest in crystal growth, there has been considerable activity in characterizing atomic behavior on close-packed fcc (111) surfaces, especially of iridium [2], platinum [3,4], and also silver [5,6]. So far, however, no information at all is available about single atom diffusion on hcp crystals [7]. As part of a larger effort to examine diffusion on densely packed planes, we have therefore carried out an exploratory survey of migration on the Re(0001) plane, in which we have examined the behavior of individual rhenium atoms as well as atom clusters, using a low-temperature field ion microscope.

In hcp crystals, close-packed (0001) planes are stacked in an ABAB sequence. As shown in Fig. 1, this stacking creates two inequivalent three-fold hollow sites, at which metal adatom binding is likely. A lattice atom is located directly underneath each hcp binding site. Thus, placing an atom on the hcp site continues the ABAB sequence. Underneath the fcc site, there is no lattice atom

* Corresponding author. Present address: Air Force Research Lab/MLPO 3005 P-Street Suite 6, Wright Patterson AFB, Dayton, OH 45433-7707, USA. Tel.: +1-937-255-4588; fax: +1-937-255-4913.

0039-6028/99/$ - see front matter
PII: S0039-6028(99)00950-4

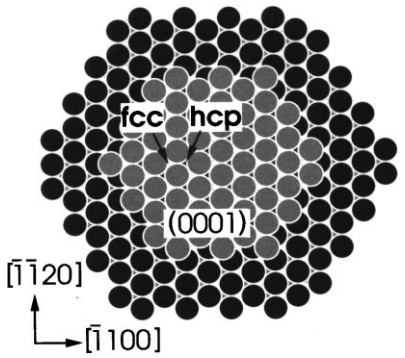

Fig. 1. Hard-sphere model of outermost layers of a [0001] oriented hcp sample, showing fcc and hcp sites. A layers in gray, B layers in black.

present throughout the entire depth of the perfect crystal. Placing an atom at the fcc site initiates an fcc ABCABC stacking sequence. When comparing these two crystal types, with no adatoms present, we find that their outermost surface layer, and the layer directly underneath it are identical. It is only in the third layer from the surface that fcc and hcp lattices differ. For Pt and Ir it has been demonstrated that around room temperature the (111) planes are not reconstructed, but the outermost layer spacing differs from that of the bulk [8–10]. Although no detailed structural studies have been reported for the basal plane of Re, there is no indication of reconstruction. In view of the structural similarities, it is therefore reasonable to expect similarities in atomic behavior on hcp(0001) and fcc(111) surfaces.

2. Sample preparation and imaging

Surfaces for field ion imaging were prepared from [0001] oriented rhenium single crystal wire (from Field Electron and Ion Sources, McMinville, OR), 0.005 in. in diameter, spot welded onto a standard tungsten hairpin equipped with potential leads for resistance thermometry. Electro-polishing methods described by Liu were used to obtain sharply pointed tips [11]. Initial thinning is accomplished at 2 V AC in a fresh mixture of four parts glycolic acid, four parts nitric acid, and three parts hydrofluric acid. Sharpening is done in an electrolyte made of four parts phosphoric acid, one part ethyl alcohol, one part glycerin, and one part hydrofluric acid, at 1.5 V AC.

Final processing of the surface proceeds after the tip assembly has been mounted in one of our low-temperature field ion microscopes [12] and UHV conditions have been achieved. After extensive heating at 750 K, the tip was sputtered with Ne^+, both to clean the surface and to sharpen the tip. This was done by drawing a current of field emitted electrons at 10^{-6} A into Ne at a pressure of 6×10^{-4} Torr. An atomically smooth surface was then prepared by field evaporation. At 20 K, it was found that field evaporation proceeds unpredictably, with sudden changes in the surface. We therefore adopted a two-step procedure, in which first approximately 50 (0001) layers are field evaporated at 200 K, with an equal number subsequently removed at 70 K.

Field ion imaging in our laboratory is typically done using helium with the surface at ca 20 K. For rhenium, the contrast between the plane edges and the central region of the (0001) plane is so great under these conditions that adatoms at the center of the plane are difficult to discern. Therefore, in this study, the surface temperature during imaging is maintained at ca 50 K by resistive heating of the support loop. By raising and lowering the image field about 100 times with the surface at 50 K it was possible to establish that the location of a rhenium adatom was not perceptibly affected during imaging under these conditions. That the orientation of the surface corresponds to that in the model in Fig. 1 was ascertained by imaging the six bright zone line decorations [13–16], which emanate from the (0001) planes, and also by identifying the location of planes peripheral to the (0001), based on the field emission pattern of the sample [11,14,17].

Tungsten and rhenium adatoms were deposited on the surface from electrically heated wire evaporators, which were maintained at $\sim$1000 K between experiments. Prior to each experiment, the evaporators were additionally cleaned by repeated heating to evaporation temperatures, and the sources were checked by monitoring the diffusion behavior of the deposited adatoms.

3. Adatoms on Re(0001)

3.1. Binding sites

The identification of binding sites occupied by adatoms on the (111) planes of Ir and Pt has been considerably simplified by the fact that individual metal atoms deposited on these surfaces produce a triangular image spot, with an orientation characteristic of the type of site [2,18,19]. On Re(0001) no such triangular images have been found, either for Re or W adatoms, even though a wide range of surface temperatures and imaging fields has been explored.

However, by repeated observation of an adatom after it has diffused over the surface it is possible to map out the binding sites occupied on the surface. Two such maps, one obtained for rhenium adatoms, the second for W adatoms on Re(0001), are shown in Fig. 2. The grid which best describes the location of the adatoms is clearly tetragonal, with adatoms found only at the intersection of the grid lines; there is no indication of adatoms in the interior of the unit cell. These maps are characteristic of a close-packed surface on which only one type of binding site, either hcp or fcc, is consistently occupied. For an hcp crystal, fcc sites in successive (0001) layers are positioned on top of each other; hcp sites, however, alternate in location from one layer to the next. The possibility therefore exists of identifying the type of site occupied by mapping the adatom location on the (0001) plane, then field evaporating it and locating the binding sites in the fresh layer exposed. In our experiments the superimposed images of adatoms on successive planes were not well enough resolved to allow an unequivocal decision about the nature of the sites occupied; nevertheless, it is clear that only one type of site is consistently favored.

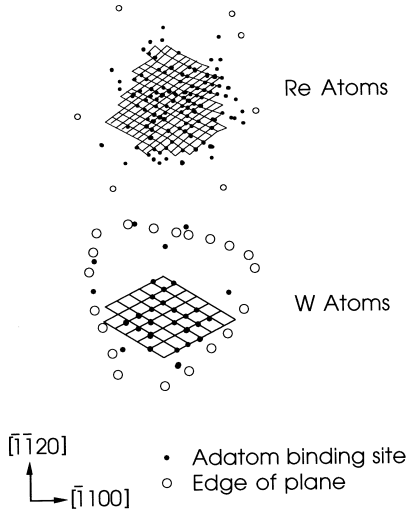

Fig. 2. Site maps for Re(0001), obtained by observing location of atoms after diffusion in absence of applied field. Sites for rhenium adatoms, on top, and for W atoms, on bottom, both form a tetragonal grid.

3.2. Diffusion of adatoms

To determine the diffusivity D of adatoms on Re(0001) we take advantage of the Einstein relation [20]

$$\langle \Delta x^2 \rangle_\infty = 2Dt, \tag{1}$$

where $\langle \Delta x^2 \rangle_\infty$ is the mean-square displacement of an adatom on an infinite surface during a time interval t. Repeated observations (M in number) of displacements over the surface made by a single adatom in the absence of any applied field provides an estimate of the mean-square displacement [21]. However, this quantity must be corrected for two different effects. The planes accessible to observation in the field ion microscope are small, for rhenium typically with a diameter on the order of 20 atom spacings. It is well established that close to the edges of a surface, the movement of adatoms is different than in the center of the plane, as the diffusion potential is distorted in the proximity of a lattice step [22–25]. Atomic displacements that take place within three atom spacings of the plane edge are therefore discarded, and the direct effects of the edges are eliminated. However, the mean-square displacement $\langle \Delta x^2 \rangle_{\text{finite}}$ derived in this way is measured on a finite surface. This displacement can be related to the value of $\langle \Delta x^2 \rangle_\infty$ appropriate for an infinite (0001) surface by an equation of the form [26,27]

$$\langle \Delta x^2 \rangle_{\text{finite}} = \langle \Delta x^2 \rangle_\infty \left[\frac{a + b\langle \Delta x^2 \rangle_\infty}{R^2} \right], \tag{2}$$

where R is the radius of the circular region in which observations of the displacement are accepted, given in terms of the nearest-neighbor distance l. From Monte Carlo simulations on (0001) planes of different radii the coefficients a and b are obtained as 0.9991 ± 0.0006 and -1.23 ± 0.03, for $\langle \Delta x^2 \rangle_{\text{finite}}$ and $\langle \Delta x^2 \rangle_{\infty}$ in units of l^2.

The second effect which must be considered when evaluating the mean-square displacement is that some diffusion occurs during temperature transients, before and after the set diffusion temperature T is reached. The extent of this diffusion is measured in zero-time experiments [28], in which heating is interrupted as soon as the set diffusion temperature is reached. The mean-square displacement, $\langle \Delta x^2 \rangle_{\text{zt}}$, calculated from M_{zt} such intervals is then subtracted from $\langle \Delta x^2 \rangle_{\infty}$, giving the final corrected mean square displacement, $\langle \Delta x^2 \rangle_{\text{f}}$. These quantities are listed in Table 1 for Re adatoms and in Table 2 for W adatoms diffusing on Re(0001). It is clear that at higher temperatures, the zero-time correction makes a significant difference.

Diffusivities of single adatoms diffusing on a surface can be represented by an Arrhenius relation [20] of the form

$$D = D_{\text{o}} \exp\left(\frac{-E_{\text{a}}}{kT}\right). \tag{3}$$

A semi-logarithmic plot of the diffusivities of single rhenium adatoms on Re(0001), shown in Fig. 3 at temperatures from 210 to 235 K, yields an activation energy E_{a} of 11.11 ± 0.43 kcal mol^{-1}, and a prefactor D_{o} of $6.13(\times 2.6^{\pm 1}) \times 10^{-6}$ cm^2 s^{-1}. For single tungsten adatoms, observations at temperatures ranging from 155 to 190 K, in Fig. 4, give an activation energy of 11.04 ± 0.34 kcal mol^{-1}, with a D_{o} of $2.17(\times 2.7^{\pm 1}) \times 10^{-3}$ cm^2 s^{-1}.

It is worth noting that diffusion of rhenium occurs at significantly higher temperatures than for tungsten adatoms, yet the activation energy for diffusion is essentially the same for the two. Differences must arise entirely from a much lower prefactor for diffusion of rhenium as compared to tungsten on Re(0001). The prefactor D_{o} for self-diffusion of rhenium adatoms on Re(0001) is surprising, more than two orders of magnitude lower than the oft-cited 'standard' value of 10^{-3} cm^2 s^{-1} [29].

Table 1
Diffusion of individual rhenium adatoms on Re(0001)

T (K)	R (l)	t (s)	M	$\langle \Delta x^2 \rangle_{\text{finite}}$	$\langle \Delta x^2 \rangle_{\infty}$	M_{zt}	$\langle \Delta x^2 \rangle_{\text{zt}}$	$\langle \Delta x^2 \rangle_{\text{f}}$
210	13	30	221	1.38 ± 0.12	1.39 ± 0.12			1.39 ± 0.12
215	13	20	359	1.62 ± 0.08	1.64 ± 0.09	122	0.004 ± 0.003	1.64 ± 0.09
225	13	20	86	4.71 ± 0.66	4.89 ± 0.72	101	0.03 ± 0.01	4.87 ± 0.72
230	13	5	67	2.33 ± 0.39	2.37 ± 0.40	96	0.29 ± 0.07	2.07 ± 0.41
235	16	5	100	7.01 ± 0.69	7.22 ± 0.74	85	3.02 ± 0.21	4.20 ± 0.77

Table 2
Diffusion of single tungsten adatoms on Re(0001)

T (K)	R (l)	t (s)	M	$\langle \Delta x^2 \rangle_{\text{finite}}$ (l^2)	$\langle \Delta x^2 \rangle_{\infty}$	M_{zt}	$\langle \Delta x^2 \rangle_{\text{zt}}$	$\langle \Delta x^2 \rangle_{\text{f}}$
155	7.6	90	126	0.14 ± 0.02	0.14 ± 0.02			0.14 ± 0.02
160	7.6	35	115	0.15 ± 0.02	0.15 ± 0.02			0.15 ± 0.02
165	7.4	15	125	0.21 ± 0.04	0.21 ± 0.04	135	0	0.21 ± 0.04
170	7.3	5	119	0.25 ± 0.03	0.25 ± 0.03	176	0.022 ± 0.006	0.23 ± 0.04
175	7.8	3	140	0.31 ± 0.04	0.31 ± 0.04	108	0.018 ± 0.008	0.29 ± 0.04
180	7.8	2	107	0.42 ± 0.06	0.42 ± 0.06	92	0.10 ± 0.03	0.32 ± 0.06
185	7.4	2	95	1.09 ± 0.12	1.12 ± 0.12	149	0.18 ± 0.03	0.94 ± 0.13
190	8.0	1	54	1.63 ± 0.22	1.68 ± 0.24	99	0.35 ± 0.06	1.34 ± 0.25

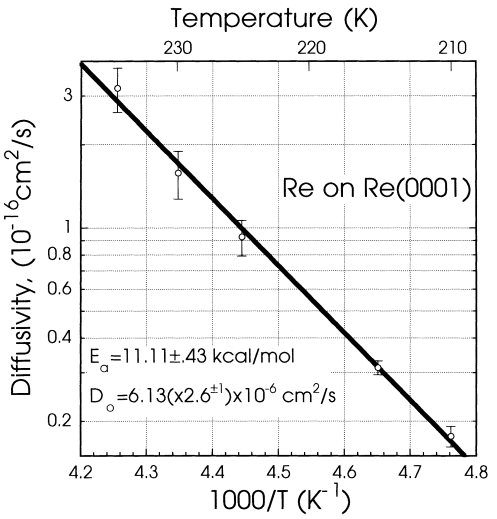

Fig. 3. Temperature dependence of the self-diffusion of single Re atoms on Re(0001), plotted as an Arrhenius relation, Eq. (3). Only the statistical uncertainties of the diffusion parameters E_a and D_o are shown.

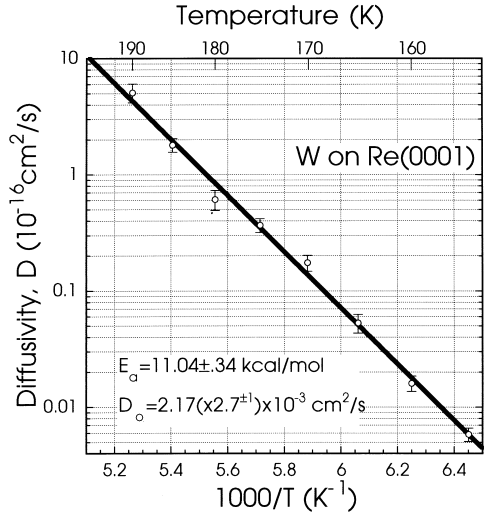

Fig. 4. Diffusivity of single tungsten atoms on Re(0001), measured in the absence of applied fields.

3.3. Step edge effects

In examining adatom diffusion, phenomena occurring close to the edges of the (0001) plane have been eliminated from consideration. For understanding how crystals actually grow, however, it is precisely these processes that are of interest, and we have therefore looked briefly at what happens when a Re or W adatom approaches the edge of the (0001) plane.

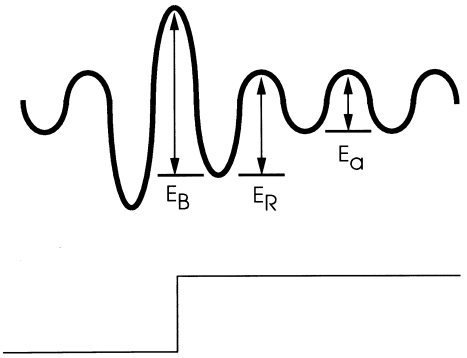

Fig. 5. Schematic of the diffusion potential for single atoms (top) in the vicinity of the edge of a Re(0001) plane, shown at bottom.

The behavior of the two different adatoms is quite similar. In migration at low temperatures, that is at $T<210$ K for W and $T<250$ K for Re, adatoms are trapped when they reach the step edge. Once trapped, they remain at the edge even on heating for 5 min at these low temperatures. If, after an adatom becomes trapped at an edge, the temperature is raised for 20 s to $T=210$ K for W or $T=250$ K for Re, the adatom will move away from the edge toward the center of the plane. This is quite a reproducible effect, observed in >50 instances.

When diffusion is allowed to occur for 2 s above these temperatures, the adatom encounters the plane boundaries many times in its peregrinations, yet it stays on the (0001) plane. However, after heating at 310 K, both Re and W disappear from the surface, presumably moving over the step edge and incorporating into the cluster. At this high temperature, the energy is sufficient to overcome the step-edge barrier which normally confines the adatom to the plane.

The overall form of the diffusion potential for Re or W adatoms at the edges of Re(0001), as inferred from our experiments, is sketched in Fig. 5. If we assume that frequency factors at the step-edge are similar to those for diffusion in the center, then the barrier E_R to returning from the edge toward the center amounts to

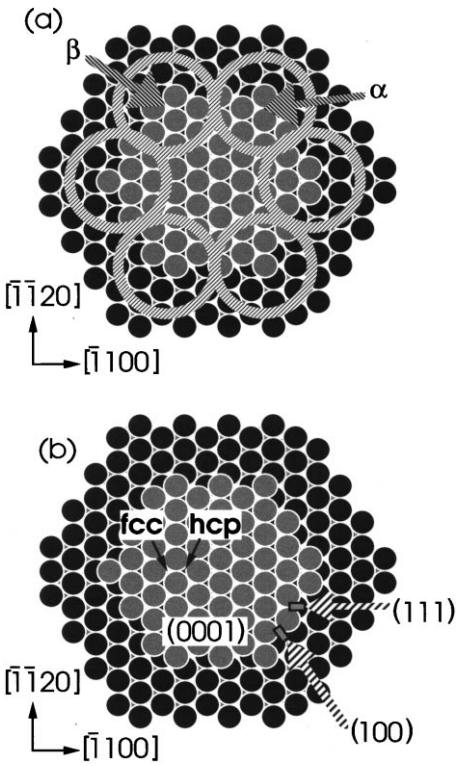

Fig. 6. Structural features of the Re(0001) plane formed by field evaporation. (a) Schematic of plane with corners encircled. The three corners found by rotating the corner labeled α through 120° around the center of the plane are identically configured. The same holds for the β-corner, formed of more highly coordinated atoms. (b) Details of edge structure. Arrow labeled (111) indicates a (111) microfacet of just three atoms, all of which border the small upper rectangle. The arrow labeled (100) indicates a (100) microfacet of four atoms which border on the lower rectangle.

13.1 ± 0.4 kcal mol^{-1} for Re and 13.4 ± 0.4 for W. The return barrier is >2 kcal mol^{-1} higher than for diffusion in the plane center. Under the same assumptions we estimate a total step-edge barrier E_B of 15.7 ± 0.4 kcal mol^{-1} for Re and 19.3 ± 0.4 for W.

Adatom behavior at the corners of the (0001) plane is unique. To appreciate this, we first note that the edges of the plane are not formed along close-packed directions, but are instead along the [1100] directions, as indicated in Fig. 6, in which the six corner sites have been circled. In a field ion image of the (0001) plane, three of the corner sites always image brightly and three dimly; in going around the edge, bright and dim corners alternate. If either a Re or W adatom reaches one of the bright corners, the adatom is localized there up to high temperatures; only at 350 K does the adatom disappear. No such peculiarly strong binding is observed in the vicinity of the dim corners. The imaging behavior is in keeping with the atomic arrangement of the corners depicted in Fig. 6. The protruding atom at a corner of type α can be expected to contribute more prominently to the field ion image, although it is not immediately obvious why binding would be favored there.

When adatoms finally incorporate after warming to $T>310$ K, what are the atomic events actually involved? On fcc(111) planes such as iridium, there are two different kinds of edges, resembling either (100) or (111) micro facets [30]. On the latter, incorporation takes place by atom exchange: an adatom on Ir(111) pushes an edge atom out and takes its place in the layer below. This has been established by placing a W adatom on the surface and then testing the identity of the adatom observed at the edge after incorporation. In an exchange process, a lattice atom will be left at the edge.

Analogous tests can be carried out on Re(0001), however the (0001) planes in the present experiments are bounded by edges of irregular, rough steps, containing small pieces of (100) and (111) microfaceted steps, as indicated in Fig. 6. Suppose a W adatom is placed on the Re(0001) plane. If incorporation occurs by jumps into the step site, then a W adatom ends up attached to the periphery. On the contrary, incorporation by exchange would leave a Re atom bound there. These possibilities are easy to distinguish, as the field-evaporation characteristics of Re and of W adatoms are quite different. W adatoms evaporate 100–300 V above the voltage giving the best adatom image. Re adatoms, on the other hand, cannot be field evaporated without at the same time removing Re atoms from the substrate.

In two experiments we have been able to examine the adatom that appears at the plane edge after depositing a W adatom and warming the surface to 310 K for 20 s. In both instances it was easy to field evaporate the adatom at the step, indicating that it was W, and that incorporation occurred in

an ordinary jump process. In view of this tiny statistical sample, there is certainly the possibility that exchange events might also occur, but the only evidence so far is for incorporation by adatoms jumping over the edge.

4. Re clusters

In diffusion experiments on macroscopic surfaces as well as in the growth of crystals, many adatoms are present on a surface. The properties of clusters formed by association of several adatoms are therefore of considerable interest, and we have briefly explored the behavior of small Re clusters of as many as eight Re adatoms on Re(0001).

4.1. Diffusion and dissociation

Clusters were created by depositing Re adatoms on the surface one at a time, and then heating to 240 K for 10 s to allow the adatoms to associate into one cluster, as illustrated in Fig. 7. When aiming at Re_6 or larger entities, two separate clusters would occasionally form. Under these circumstances, the temperature was raised in steps of 10 K for 10 s until one of the clusters became sufficiently mobile to coalesce. The octamer in Fig. 8 was formed in this way.

The temperature for the onset of diffusion of the clusters was determined by heating the surface for 10 s. After cooling to the imaging temperature, the cluster is viewed to check for any displacement. In the absence of any motion the temperature is incremented another 10 K, and the procedure is repeated until diffusion sets in. For Re_1–Re_7, these observations were done on at least three separate clusters, and mean diffusion temperatures are plotted in Fig. 9.

Dimers proved quite distinct in their behavior. They tend to dissociate at essentially the same temperature at which single Re adatoms begin to diffuse over Re(0001). Furthermore, they are much more susceptible to field evaporation than larger clusters. The most interesting feature of the size dependence is the sharp drop in the diffusion temperature for Re_4 compared to the trimer or pentamer. After the tetramer, the temperature for cluster motion rises monotonically up to the highest cluster checked, Re_8.

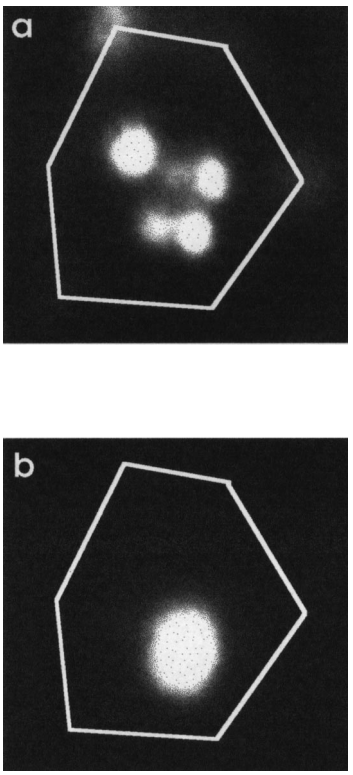

Fig. 7. Formation of rhenium pentamer on Re(0001). (a) Five Re atoms have been deposited on the Re surface maintained at 15 K. (b) After heating to 240 K for 10 s, the atoms have combined into one cluster. The faint plane edges are indicated by the hexagon in white.

Once mobility had been established for a given cluster, heating for 10 s intervals after increasing the temperature in 10 K increments was continued until the cluster disappeared from the central (0001) plane during one heating interval. In these experiments the products of dissociation were never seen, except in the case of dimers. This is expected, as the mobility of an adatom and cluster formed by dissociation is much higher than that of the parent cluster, except for dimers and tetramers. The temperatures at which Re clusters of different size disappear from Re(0001) are also plotted in Fig. 9. Activation energies for diffusion as well as for disappearance from the basal plane

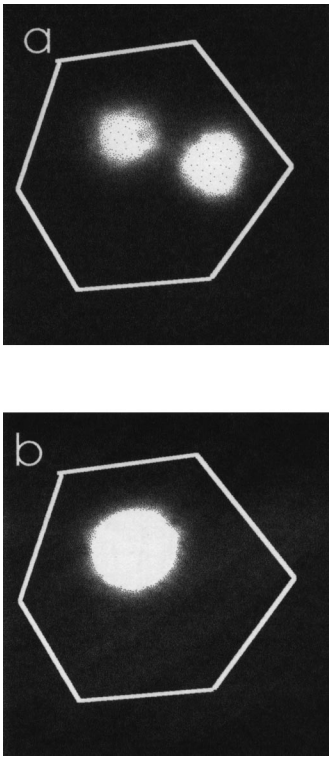

Fig. 8. Formation of Re octamer by combination of smaller clusters. (a) Separate pentamer and trimer have been produced by depositing Re atoms on Re(0001) at 15 K. (b) Heating for 10 s at 320 K causes clusters in (a) to coalesce into an octamer.

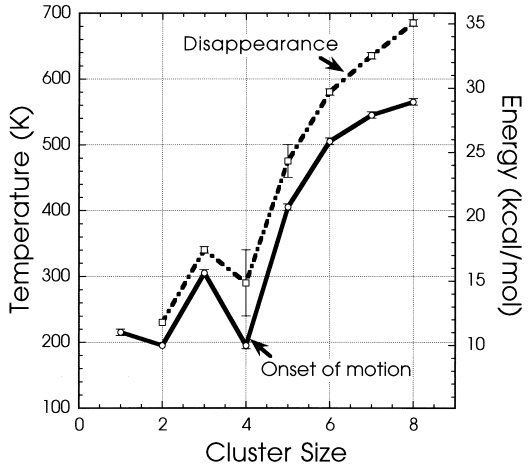

Fig. 9. Temperature for the onset of motion and for the disappearance of Re clusters of increasing size from Re(0001). Energies are derived assuming the same prefactor as for atom jumps in diffusion.

have been estimated assuming a prefactor equal to that for diffusive jumps of adatoms.

Overall, the trends in the effects of size on cluster diffusion and disappearance are quite similar. Clusters may disappear by dissociation, but there is also the possibility that they simply diffuse to the edge and escape there. Given that for all except tetramers, the RMS diffusion distance during a dissociation experiment is small compared to the plane diameter, the likelihood of a cluster's diffusing over the edge as a unit is small. The similarity in the curves for diffusion and dissociation make it seem likely that diffusion occurs by jumps of single cluster atoms, which partially sever their bonding to the rest of the cluster.

4.2. Field promoted motion

Only for tetramers are the individual cluster adatoms resolved, revealing a tetragonal arrangement. When the tetramer is imaged at 50 K, a curious phenomenon occurs when the voltage is raised ca 13% above that required for first detecting an image: the tetramer appears to spin as a unit about a static center. The rotation switches direction erratically, spinning either clockwise or counter-clockwise while imaged at a constant field. When switching directions, the tetramer pauses momentarily with its long diagonal parallel to a plane edge. Throughout all this the cluster center remains fixed in place. It appears that the imaging field lifts the tetramer off the surface a bit, as suggested in the schematic in Fig. 10, so that its center of mass is situated directly above an underlying surface atom. Bombardment by the He image gas then sets the tetramer into rotational Brownian motion.

This intriguing field effect suggests that the tetramer can move as a unit, which may help in rationalizing the unusually low temperature for tetramer diffusion in the absence of electric fields.

5. Comparisons

5.1. Self-diffusion

The results for the diffusion of Re on Re(0001) are especially interesting when viewed in compari-

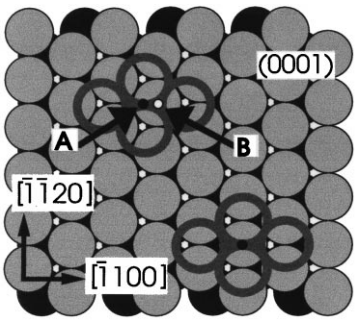

Fig. 10. Schematics of possible tetramer positions on Re(0001). (a) Re_4, with constituent adatoms located in three-fold hollows. Center of mass, marked by black circle labeled A, is slightly offset from the center of the underlying Re atom, marked by a white circle labeled B. (b) Tetramer raised out of the surface and translated so that the center lines up with the center of lattice atom below.

son with what is known about self-diffusion of sixth row metals in the periodic table in the vicinity of Re. In Table 3 are listed not only the barrier to migration E_a and prefactor D_o, but also the heat of vaporization ΔH_v for each element at 298 K (a measure of the cohesive energy) [32]. Tungsten is close to Re in cohesive energy, $\Delta H_v(W)/\Delta H_v(Re) = 1.10$; however, the activation energies for diffusion stand in the ratio of 1.91. Thus, scaling by the cohesive energy does not bring the self-diffusion barriers for Re and W into coincidence. This should not be surprising, as the (110) plane of W, although it is the densest plane of the bcc lattice, is not close packed as is Re(0001).

Comparison of Re(0001) with the (111) planes of platinum family metals is perhaps more soundly founded, in that the arrangement of the two outermost layers is the same. Despite that, surface

Table 3
Self-diffusion parameters for single atoms on densely packed planes of elements across the sixth row of the periodic table

	W(110)	Re(0001)	Ir(111)	Pt(111)
E_a (kcal mol^{-1})	21.2 ± 1.1[a]	11.11 ± 0.43[c]	6.15 ± 0.07[d]	6.00 ± 0.07[e]
D_o (cm^2 s^{-1})	2.6×10^{-3} [a]	$6.13(\times 2.6 \pm 1) \times 10^{-6}$ [c]	$9.0(\times 1.4 \pm 1) \times 10^{-5}$ [d]	$2.0(\times 1.4 \pm 1) \times 10^{-3}$ [e]
ΔH_v (kcal mol^{-1})	203[b]	184[b]	159[b]	135[b]
$E_a/\Delta H_v$	0.104	0.060	0.039	0.044

[a] Ref. [31].
[b] Ref. [32].
[c] This work.
[d] Ref. [2].
[e] Ref. [4].

Table 4
Diffusion parameters for W and Re adatoms on W(110), W(211), Ir(111) and Re(0001); $\aleph = E_a/\Delta H_v$

	E_a (kcal mol^{-1})				
	Re	W	$E_a/\Delta H_v$(Re)	$E_a/\Delta H_v$(W)	$\aleph$(Re)/$\aleph$(W)
W (110)	23.9 ± 2[a]	21.2 ± 1.1[b]	0.130	0.104	1.25
W (211)	19.2 ± 0.5[c]	19.0 ± 0.6[c]	0.104	0.094	1.11
Ir (111)	12.00 ± 0.17[d]	11.69 ± 0.27[d]	0.065	0.058	1.12
Re (0001)	11.11 ± 0.43[e]	11.04 ± 0.34[e]	0.060	0.054	1.11

[a] Ref. [34].
[b] Ref. [31].
[c] Ref. [21].
[d] Ref. [2].
[e] This work.

diffusion on Re(0001) and Ir(111) is quite different. The ratio of diffusion barriers is 0.6, compared to a cohesive energy ratio of 0.86; for the self-diffusion of platinum atoms $E_a(Pt)/E_a(Re)=0.54$, while $\Delta H_v(Pt)/\Delta H_v(Re)=0.733$. For self-diffusion, scaling the diffusion barrier using the cohesive energies does not appear to afford quantitative predictions, except possibly for most closely related elements, such as Pt and Ir.

The prefactor D_o for diffusion of Re on Re(0001) is also unusual, amounting to $<10^{-5}\,cm^2\,s^{-1}$, compared to a figure closer to $10^{-3}\,cm^2\,s^{-1}$ for the other metals in Table 3. The magnitude of the prefactor depends specifically upon the vibrational frequencies of the particular system. Short of a detailed vibrational analysis, which is not available, it is difficult to make significant correlations to rationalize this apparently low value. However, it is interesting that on Ir(111), prefactors tend to be on the low side [2].

For single Re adatoms on Re(0001), diffusion appears rather different from that of its near neighbors in the periodic table. It is therefore surprising that, in some ways, Re clusters on Re(0001) behave much the same as Ir clusters on Ir(111) [33]. The trends as the cluster size increases are quite similar on Re and Ir, both in diffusion and in disappearance; even the absolute magnitudes of the diffusion barriers are quite close. Most interesting is the pronounced dip observed in the barriers for tetramers in both materials.

5.2. Diffusion of Re and W on different surfaces

The chemical specificity of the measured prefactors to diffusion for rhenium and tungsten on Re(0001) contrast sharply with the similarity of their activation energies listed in Table 4. On Re(0001), Ir(111), as well as W(211), the activation energies for diffusion of Re and of W adatoms on a specified plane are quite close to each other. Scaling the barrier heights by the cohesive energies of Re or W (in the solid) actually accentuates the difference between the two adatoms. The ratio of the scaled barriers for Re as compared to W is reasonably constant on these planes, and amounts to $\sim$1.11. Such trends do not seem to hold for W(110). However, these are very early measurements on W(110), and it will be interesting to see if newer and more extensive measurements will reveal such empirical comparisons as useful.

6. Summary

Although Re and W are neighbors in the periodic table, atomic behavior on the close-packed Re(0001) plane has little in common with that on the (110) plane of W, its most densely packed plane. There are much greater similarities between the diffusion on Re(0001) and Ir(111), for which the structure of the two outermost layers is the same. Nonetheless, empirical extrapolations fail to adequately describe single adatom diffusion on Re(0001).

Acknowledgements

This work was supported by the U.S. Department of Energy, Division of Materials Sciences, under Grant No. DEFG02-96ER-45439 through the Materials Research Lab. J.G. wishes to acknowledge the encouragement of his Air Force Monitor Dr. Patrick Hemenger, as well as the generous financial support of the Air Force through the Senior Knight Program.

References

[1] G. Ehrlich, in: M.C. Tringides (Ed.), Surface Diffusion: Atomistic and Collective Processes, Plenum Press, New York, 1997, p. 23.
[2] S.C. Wang, G. Ehrlich, Phys. Rev. Lett. 68 (1992) 1160.
[3] M. Bott, M. Hohage, M. Morgenstern, T. Michely, G. Comsa, Phys. Rev. Lett. 76 (1996) 1304.
[4] K. Kyuno, A. Gölzhäuser, G. Ehrlich, Surf. Sci. 397 (1998) 191.
[5] H. Brune, K. Bromann, H. Röder, K. Kern, J. Jacobsen, P. Stoltze, K. Jacobsen, J. Nørskov, Phys. Rev. B 52 (1995) 14380.
[6] K. Bromann, H. Brune, H. Röder, K. Kern, Phys. Rev. Lett. 75 (1995) 677.
[7] G. Kellog, Surf. Sci. Rep. 21 (1994) 1.
[8] M. Hohage, T. Michely, G. Comsa, Surf. Sci. 337 (1995) 249.

[9] G. Grübel, K.G. Huang, D. Gibbs, D.M. Zehner, A.R. Sandy, S.G.J. Mochrie, Phys. Rev. B 48 (1993) 18119.
[10] P.R. Watson, M.A. Van Hove, K. Herman, Atlas of surface structures, J. Phys. Chem. Ref. Data Monograph 5 (1994)
[11] R. Liu, PhD. Thesis, University of Illinois at Urbana Champaign, 1977.
[12] D.A. Reed, G. Ehrlich, Surf. Sci. 151 (1985) 143 equipment standard in authors' laboratory.
[13] K.M. Bowkett, D.A. Smith, Field-Ion Microscopy, North-Holland, Amsterdam, 1970.
[14] E.W. Müler, T.T. Tsong, Field Ion Microscopy, Elsevier, New York, 1969.
[15] A.J. Melmed, Surf. Sci. 5 (1966) 359.
[16] A.J. Melmed, Surf. Sci. 8 (1967) 191.
[17] R. Gomer, Field Emission and Field Ionization, Harvard University Press, Cambridge, 1961.
[18] S.C. Wang, G. Ehrlich, Surf. Sci. 246 (1991) 37.
[19] S.C. Wang, G. Ehrlich, J. Chem. Phys. 94 (1991) 4071.
[20] J.R. Manning, Diffusion Kinetics for Atoms in Crystals, van Nostrand, Princeton, NJ, 1968.
[21] S.C. Wang, G. Ehrlich, Surf. Sci. 206 (1988) 451 techniques for data analysis.
[22] K. Kyuno, G. Ehrlich, Surf. Sci. 394 (1997) L179.
[23] H.-W. Fink, G. Ehrlich, Surf. Sci. 143 (1984) 125.
[24] S.C. Wang, G. Ehrlich, Phys. Rev. Lett. 71 (1993) 4174.
[25] S.C. Wang, G. Ehrlich, Phys. Rev. Lett. 70 (1993) 41.
[26] G. Ehrlich, J. Chem. Phys. 44 (1966) 1050.
[27] D.A. Reed, G. Ehrlich, Surf. Sci. 120 (1982) 179.
[28] M.F. Lovisa, G. Ehrlich, Surf. Sci. 246 (1991) 43.
[29] C.P. Flynn, in: Point Defects and Diffusion, Clarendon Press, Oxford, 1972, pp. 306–374.
[30] S.C. Wang, G. Ehrlich, Phys. Rev. Lett. 67 (1991) 2509.
[31] G. Ayrault, G. Ehrlich, J. Chem. Phys. 60 (1974) 281.
[32] D.R. Lide (Ed.), Handbook of Chemistry and Physics, CRC Press, Boca Raton, FL, 1996, pp. 4–5.
[33] S.C. Wang, G. Ehrlich, Surf. Sci. 239 (1990) 301.
[34] D.W. Bassett, M.J. Parsley, J. Phys. D 3 (1970) 707.